Supporting Information

Impact of aggregate formation

on the viscosity of protein solutions

Lucrèce Nicoud, Marco Lattuada, Andrew Yates, Massimo Morbidelli*
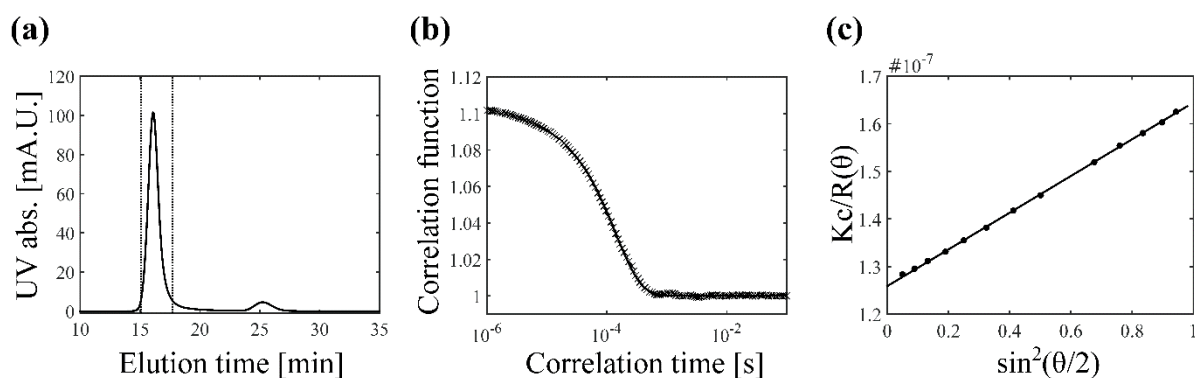
1. Experimental results

Figure S1: (a) Representative SEC chromatogram, obtained for a sample incubated 35 min at the protein concentration of 40 g/L. The portion of the chromatogram used for aggregate characterization by inline light scattering is comprised between the two dotted lines, i.e. between 15.1 and 17.7 min. (b) Correlation function measured by inline dynamic light scattering at the elution time of 16 min of the shown chromatogram. The minimum and maximum thresholds for data processing were set to 5 and 300 nm, respectively. The fit of the autocorrelation function (line) is compared to experimental data (crosses) (c) Results from static light scattering measurements at the elution time of 16 min of the shown chromatogram analyzed with the Astra software.
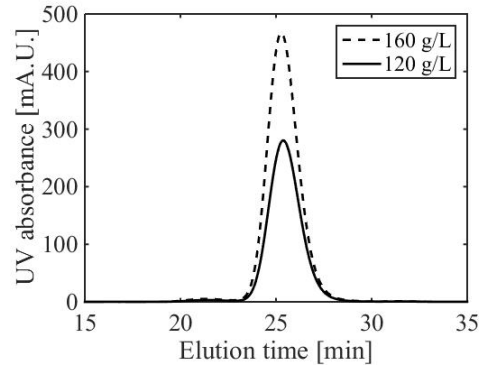
Figure S2: SEC chromatograms of non-heated antibody samples at protein concentrations of 120 and 160 g/L, showing that the antibody remains monomeric at high concentration under native conditions.
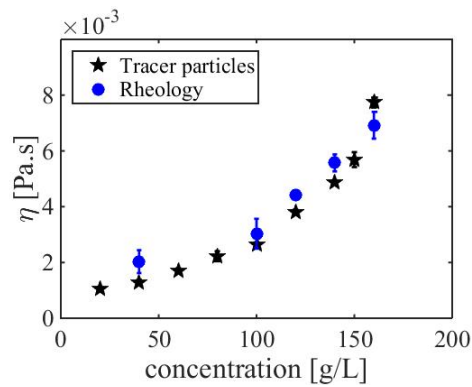

Figure S3: Comparison between viscosity results obtained from the diffusion coefficient of tracer nanoparticles with DLS, and viscosity results obtained from rheological measurements. Rheological measurements were performed with a Physica MCR 300 rheometer (Paar Physica) by using a cone-and-plate geometry (12.5 mm radius, 2° angle). The gap was set to 0.05 mm and the sample volume was 160 µL. The temperature was maintained at 25 °C by a Peltier element (TEK 150 PA-C). Viscosity measurements were performed at 1000 s^{-1} on three independent samples.
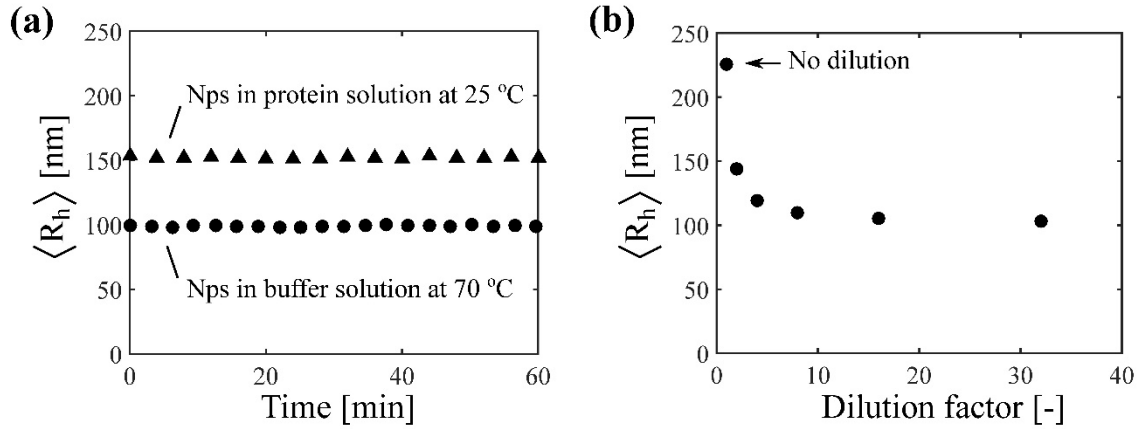
Figure S4: (a) Apparent hydrodynamic radius of the tracer nanoparticles (Nps) as a function of time in the buffer solution at 70 °C, and in a protein solution at the concentration of 40 g/L at 25 °C. It is seen that the nanoparticles are stable in both cases. (b) Apparent hydrodynamic radius of the tracer nanoparticles as a function of the dilution factor for a mAb sample that was incubated in the presence of the nanoparticles at 70 °C and at the protein concentration of 40 g/L. Measurements of the tracer particle size at various dilutions were performed at room temperature on the quenched sample. It seen that when the sample in sufficiently diluted in order to reach the solvent viscosity, a hydrodynamic radius of 100 nm is measured, which corresponds to the primary particle size. This shows that the nanoparticles are stable during mAb aggregation.
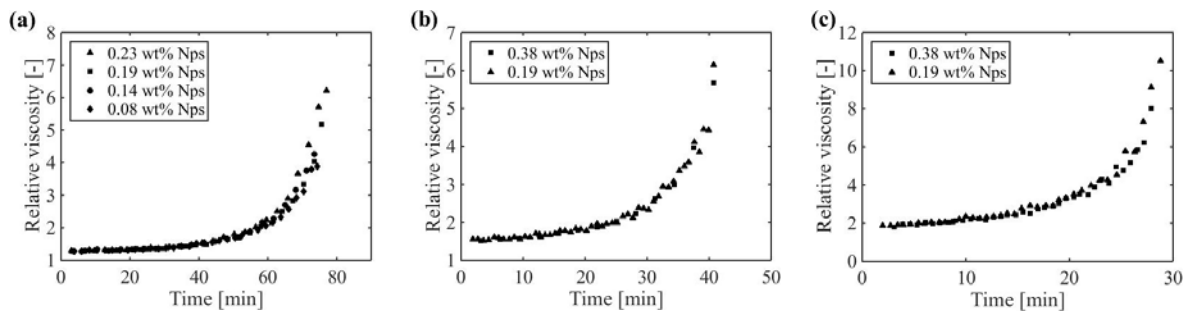

Figure S5: Kinetics of the increase in viscosity measured with different nanoparticle concentrations (as indicated in the legends) at protein concentrations of (a) 20 g/L, (b) 40 g/L, (c) 60 g/L. This set of experiments shows that the viscosity results are independent of the concentration of nanoparticles (in the range of concentrations investigated).
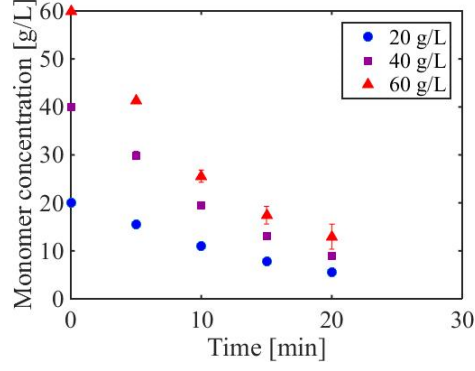
Figure S6: Monomer depletion measured with SEC at three protein concentrations, as indicated in the legend.

2. Boundaries for the volume fraction

In the following, we show that the approximate volume fraction φ defined in the main text provides a lower bound of the exact volume fraction ϕ when the number average radius is considered.

We recall that the exact and approximate volume fractions were defined respectively as:

$$\phi = \frac{4}{3}\pi \sum_i N_i R_{h,i}^3 \tag{1}$$

$$\varphi = \frac{4}{3}\pi \frac{N_0}{k_f} R_p^{d_f} \langle R_h \rangle^{3-d_f} \tag{2}$$

Where N_i and $R_{h,i}$ are the number concentration and hydrodynamic radius, respectively, of the aggregates containing i primary particles. R_p denotes the primary particle radius, while $\langle R_h \rangle$ stands for the average hydrodynamic radius. The parameters d_f and k_f are the aggregate fractal dimension and scaling prefactor, respectively. N_0 denotes the initial protein concentration and is also equal to:

4

$$N_0 = \sum_i i N_i \qquad (3)$$

The initial volume fraction is:

$$\phi_0 = \frac{4}{3} \pi R_p^3 N_0 \qquad (4)$$

It can be noticed that:

$$\varphi = \phi_0 \frac{1}{k_f} \times \left(\frac{\langle R_h \rangle}{R_p} \right)^{3-d_f} \qquad (5)$$

We define the number, surface and volume average hydrodynamic radii respectively as:

$$\begin{cases} \langle R_N \rangle = \dfrac{\sum_i N_i R_i}{\sum_i N_i} \\ \langle R_S \rangle = \dfrac{\sum_i N_i R_i^2}{\sum_i N_i R_i} \\ \langle R_V \rangle = \dfrac{\sum_i N_i R_i^3}{\sum_i N_i R_i^2} \end{cases} \qquad (6)$$

Moreover, we introduce r_i and n_i defined as:

$$\begin{cases} r_i = \dfrac{R_i}{\langle R_N \rangle} \\ n_i = \dfrac{N_i}{\sum_i N_i} \end{cases} \qquad (7)$$

By combining equations (1) and (3)-(6), it follows that:

$$\phi = \phi_0 \frac{\langle R_N \rangle \langle R_S \rangle \langle R_V \rangle}{R_p^3} \times \frac{\sum_i N_i}{\sum_i i N_i} \qquad (8)$$

We try to find an upper bound for A defined as:

5

$$A = \frac{\sum_i i N_i}{\sum_i N_i} = \sum_i i n_i \tag{9}$$

According to the fractal scaling, aggregate mass is connected to aggregate radius by:

$$i = k_f \left(\frac{R_{h,i}}{R_p} \right)^{d_f} \tag{10}$$

Therefore:

$$A = \sum_i k_f \left(\frac{R_{h,i}}{R_p} \right)^{d_f} n_i \tag{11}$$

Let us recall the theorem of norm monotonicity. For a series of numbers x_i weighted by coefficients w_i such as $\sum_i w_i = 1$ and for two non-zero real numbers p and q such as $p \leq q$:

$$\left(\sum_i w_i x_i^{\,p} \right)^{1/p} \leq \left(\sum_i w_i x_i^{q} \right)^{1/q} \tag{12}$$

Since $d_f \leq 3$, and $\sum_i n_i = 1$, it follows:

$$\sum_i r_i^{d_f} n_i \leq \left(\sum_i r_i^{3} n_i \right)^{d_f/3} \tag{13}$$

It follows that:

$$\sum_i r_i^{d_f} n_i \leq \sum_i r_i^{3} n_i \tag{14}$$

$$\sum_i {R_i}^{d_f} n_i \leq \left(\sum_i R_i^3 n_i \right) \langle R_N \rangle^{d_f - 3} \tag{15}$$

$$\sum_i {R_i}^{d_f} n_i \leq \langle R_N \rangle \langle R_S \rangle \langle R_V \rangle \langle R_N \rangle^{d_f - 3} \tag{16}$$

$$A \leq \frac{k_f}{R_p^{d_f}} \langle R_N \rangle \langle R_S \rangle \langle R_V \rangle \langle R_N \rangle^{d_f - 3} \tag{17}$$

Therefore,

$$\phi \geq \phi_0 \frac{\langle R_N \rangle \langle R_S \rangle \langle R_V \rangle}{R_p^3} \times \frac{1}{\dfrac{k_f}{R_p^{d_f}} \langle R_N \rangle \langle R_S \rangle \langle R_V \rangle \langle R_N \rangle^{d_f - 3}} \tag{18}$$

$$\phi \geq \phi_0 \frac{1}{k_f} \times \left(\frac{\langle R_N \rangle}{R_p} \right)^{3 - d_f} \tag{19}$$

Equations (5) and (19) show that $\phi \geq \varphi$ provided that $\langle R_h \rangle = \langle R_N \rangle$. In other words, the estimated occupied volume fraction is underestimated when computed from the number average hydrodynamic radius.

Using a similar procedure, it is possible to provide an upper boundary to the volume fraction. In order to obtain the required result, we can proceed as follows. We introduce r_i and n_i defined now as:

$$\begin{cases} r_i = \dfrac{R_i}{\langle R_V \rangle} \\ n_i = \dfrac{N_i}{\sum_i N_i} \end{cases} \tag{20}$$

This time, we will find a lower boundary for the quantity A, defined by Equation (11).

By applying equation (12) to r_i between 1 and d_f, it follows:

$$\sum_i r_i^{d_f} n_i \geq \left(\sum_i r_i n_i \right)^{d_f} \geq \left(\sum_i r_i n_i \right) \tag{21}$$

This implies that:

$$\sum_i R_i^{d_f} n_i \geq \left(\sum_i R_i n_i \right) \langle R_V \rangle^{d_f-1} = \langle R_N \rangle \langle R_V \rangle^{d_f-1} \tag{22}$$

Therefore:

$$A \geq \frac{k_f}{R_p^{d_f}} \langle R_N \rangle \langle R_V \rangle^{d_f-1} \tag{23}$$

By inserting this inequality in Equation (8), we obtain:

$$\phi \leq \frac{\phi_0}{k} \frac{\langle R_S \rangle \langle R_V \rangle^{2-d_f}}{R_p^{3-d_f}} \tag{24}$$

Finally, the surface average size is smaller than the volume average size. Therefore:

$$\phi \leq \frac{\phi_0}{k_f} \frac{\langle R_V \rangle^{3-d_f}}{R_p^{3-d_f}} \tag{25}$$

To conclude, the real value of the volume fraction is comprised between the one evaluated using the number-average size and the one evaluated using the volume average size.

8